Quantitative Characterization of Weak Self-Association in Concentrated Solutions of Immunoglobulin G via the Measurement of Sedimentation Equilibrium and Osmotic Pressure†

Mercedes Jiménez,‡ Germán Rivas,‡ and Allen P. Minton*,§

Department of Protein Science, Centro de Investigaciones Biológicas, Consejo Superior de Investigaciones Científicas, E-28040 Madrid, Spain, and Laboratory of Biochemistry and Genetics, National Institute of Diabetes and Digestive and Kidney Diseases, National Institutes of Health, U.S. Department of Health and Human Services, Bethesda Maryland 20892-0830

Received March 21, 2007; Revised Manuscript Received May 7, 2007

ABSTRACT: The sedimentation equilibrium of solutions of immunoglobulin G in saline buffer, over a concentration range up to 125 g/L, was measured and analyzed in the context of a model that takes into account the possibility of attractive intermolecular interaction leading to the reversible formation of oligomeric species and repulsive intermolecular interaction leading to nonideal solution behavior. Additionally, previously published data on the concentration dependence of the osmotic pressure of immunoglobulin G under similar conditions, over a concentration range up to 400 g/L, were analyzed in the context of a newly developed thermodynamic formalism describing the osmotic pressure of a solution containing multiple nondiffusible solute species at an arbitrary concentration. Both sets of data are quantitatively accounted for by a model in which IgG self-associates at very high concentration to form (predominantly) trimers under the conditions of these experiments.

The study of protein behavior in highly concentrated or volume-occupied solutions is essential to a complete understanding of how proteins function within crowded biological fluids (*1*) and how the stability and efficacy of protein biopharmaceuticals may be affected by storage and administration of highly concentrated solutions (*2*). The detection and quantitative characterization of weak associations leading to the formation of protein complexes that may be present only in concentrated or crowded solutions presents both experimental and theoretical challenges to the investigator because of the enhanced contribution of nonspecific repulsive protein−protein interactions (e.g., steric exclusion) to the behavior of proteins in such solutions (*3*) that tend to obscure the presence of the attractive interactions of interest. The technique of nonideal tracer sedimentation equilibrium was developed specifically to detect these weak hidden associations, and the application of this technique has revealed significant self-association of ovalbumin (*4*), aldolase (*4*), and ribonuclease (*5*) that is detectable only at concentrations in excess of 30 g/L, that is, well above concentrations at which most physical−chemical measurements of proteins in solution are carried out.

The properties of concentrated solutions of immunoglobin G (IgG[1]) are of special interest, as many protein biopharmaceuticals are engineered monoclonal IgGs (*6*). We have measured the sedimentation equilibrium of saline solutions of human IgG over a concentration range up to 125 g/L and have analyzed the data in the context of a model that takes into account the presence of both attractive interactions leading to reversible association and repulsive interactions leading to nonideal solution behavior (*5*). In addition, we reanalyzed previously published data on the concentration dependence of the osmotic pressure of solutions of bovine IgG, obtained over a concentration range up to 400 g/L (*7*), and show that these data may be accounted for quantitatively by the same model for attractive and repulsive interactions that best accounts for our sedimentation equilibrium data.

MATERIALS AND METHODS

Immunoglobulin G from human serum was obtained from Sigma-Aldrich as reagent grade lyophilized powder and used without further purification. The protein was equilibrated by extensive dialysis in phosphate-buffered saline (0.05 M sodium phosphate and 0.15 M NaCl at pH 7.4).

Mathematical simulation and modeling were carried out using scripts written in MATLAB (R2006B, Mathworks, Natick, MA), which are available upon request.

Measurement of Sedimentation Equilibrium. At low (<5 g/L) protein concentrations, the sedimentation equilibrium experiments were performed in an Optima XL-A analytical ultracentrifuge (Beckman-Coulter Inc., Fullerton, CA) equipped with a UV−vis detector system, using double-sector 12-mm centerpieces of Epon-charcoal. IgG samples (70 μL) were centrifuged at low speed (5000−8000 rpm) and 20 °C. Absorbance gradients were measured at 280 and/or 250 nm, depending upon protein concentration. After acquisition of

† This work was supported in part by Grant BFU2005-04087-C02-01 from the Spanish Science and Education Ministry to G.R. and by the Intramural Research Program of the National Institute of Diabetes and Digestive and Kidney Diseases.

* To whom correspondence should be addressed. Dr. Allen P. Minton, Building 8, Room 226, NIH, Bethesda, MD 20892-0830. Tel: (301) 496-3604. Fax: (301) 402-0240. E-mail: minton@helix.nih.gov.

‡ Consejo Superior de Investigaciones Científicas.

§ U.S. Department of Health and Human Services.

[1] Abbreviation: IgG, immunoglobulin G.

10.1021/bi7005515 CCC: $37.00
Published on Web 06/23/2007

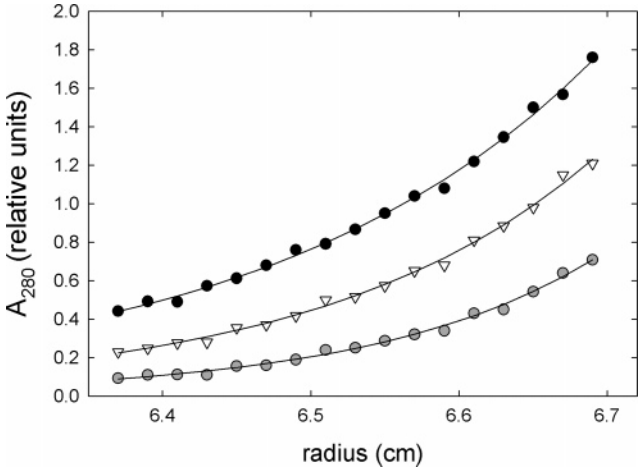

FIGURE 1: Representative concentration gradients of IgG at sedimentation equilibrium, measured as described in the text, plotted together with the corresponding best fit of eq 1. (○): loading concentration 25 g/L; best fit $M^*_{w,app}$ = 34,400. (▽): loading concentration 50 g/L; best fit $M^*_{w,app}$ = 29,100. (●): loading concentration 100 g/L; best fit $M^*_{w,app}$ = 23,000.

the equilibrium gradient, the samples were centrifuged at high speed (ca. 50 000 rpm) to deplete the meniscus and estimate baseline corrections. At high (>5 g/L) protein concentrations, 70 μL samples were centrifuged at 20 °C and 6000 rpm to sedimentation equilibrium in an Optima Max XL preparative ultracentrifuge (Beckman-Coulter) using small polycarbonate tubes and a TLS-55 rotor as described earlier (*8*). In order to measure the equilibrium gradient of protein immediately after the conclusion of centrifugation, the contents of each tube were fractionated with a BRANDEL FR-115 centrifuge tube microfractionator (BRANDEL Corp. Gaithersburg, MD) as described in Darawshe et al. (*8*), and the relative protein concentration in each fraction was determined by measurement of the absorbance at 280 nm following dilution of the fractions in buffer to a final absorbance between 0.2 and 1.0 OD units, as previously described (*5*). High-speed depletion runs were done in parallel to determine baseline signals. All experiments were conducted in triplicate.

The measured equilibrium concentration (signal) gradient obtained for each loading concentration was fit by the following equation:

$$s(r) = s(r_o)\exp\left[\frac{M^*_{w,app}\,\omega^2}{2RT}(r^2 - r_o^2)\right] \quad (1)$$

where r_o denotes an arbitrarily selected reference position, ω the angular velocity, R the molar gas constant, T the absolute temperature, and $M^*_{w,app}$ the apparent weight-average buoyant molar mass, which is an average over the solution column and is assumed to be characteristic of the composition of the loading solution (*9*). Values of $M^*_{w,app}$ subsequently utilized for analysis as described below were the mean of the values obtained by independent fitting of eq 1 to the gradient obtained from each of the three replicate experiments conducted for a given protein concentration. Examples of best-fits of eq 1 are plotted together with the corresponding data sets in Figure 1.

Model Calculation of Concentration Dependence of Solution Composition. In the present work, we explicitly consider a solution containing monomer A in equilibrium with one or more oligomers A_2, A_3, ..., with equilibrium association constants

$$K_i^0 \equiv \frac{a_i}{a_1^i} = \frac{\gamma_i c_i}{\gamma_1^i c_1^i} \quad (2)$$

where a_i, γ_i, and c_i denote the thermodynamic activity, activity coefficient, and molar concentration, respectively, of i-mer. It follows that the concentrations of the monomer and each oligomer are related by apparent equilibrium association constants as follows.

$$K_i = \frac{c_i}{c_1^i} = K_i^0\frac{\gamma_1^i}{\gamma_i} = K_i^0\Gamma_i \quad (3)$$

The activity coefficients, which are a measure of the free energy of nonspecific interaction between solute molecules arising from volume exclusion and electrostatic repulsion between protein molecules bearing like charges, are calculated as a function of solution composition using relationships obtained from an effective hard particle model described elsewhere (*3*, *10*). According to this model, each macromolecular species is represented by an equivalent hard convex particle (such as a sphere) whose size is related to its mass via a specific volume υ_{eff}, the magnitude of which reflects both volume exclusion and nonspecific electrostatic repulsions and attractions (*1*). The nonideality correction factors Γ_i approach a value of 1 in the ideal solution limit (low total protein concentration) but may become substantially greater than 1 at high total protein concentration (*3*). At high total protein concentration, the thermodynamic activity and composition become mutually interdependent, and hence the composition must be computed iteratively as described previously by Chatelier and Minton (*10*), Snoussi and Halle (*11*), and Zorrilla et al. (*5*). The procedure is summarized as follows: (1) A value of υ_{eff} is specified. (2) The value of c_{tot} is set equal to w_{tot}/M_1. (3) Initial values of K_i are set equal to K_i^0. (4) The equation of conservation of mass

$$c_{tot} = c_1 + \sum_i iK_i c_1^i \quad (4)$$

(where the summation is over all species postulated in a given model) is solved numerically for c_1, and c_i are then calculated via eq 3. (5) The concentration of each i-mer is converted to the number densities (#/cm^3) using the following equation:

$$\rho_i = c_i N_A/1000 \quad (5)$$

where N_A denotes Avogadro's number. (6) The values of ln γ_i are calculated from ρ_i and υ_{eff} using relationships specified by the effective hard particle model (*10*) with each species represented as an effective sphere. (7) The apparent equilibrium constants are recalculated according to the following equation:

$$\ln K_i = \ln K_i^0 + i\ln\gamma_1 - \ln\gamma_i \quad (6)$$

Steps 4−7 are repeated iteratively until the values of all c_i converge. Our criterion of convergence is that the concentrations of all species remain constant to within one part in 1000 between successive iterations.

The concentrations of each species may then may be expressed in w/v units (g/L).

$$w_i = c_i M_i \tag{7}$$

Model Calculation of Apparent Weight-Average Buoyant Molar Mass. The buoyant mass of each species is defined as follows:

$$M_i^* = M_i\left(\frac{\partial D}{\partial w_i}\right)_\mu \tag{8}$$

where D denotes the density of the solution, and the subscript μ indicates that the derivative quantity is taken under conditions such that the chemical potential of all other solutes (e.g., salts) is constant (*12*). Because all macrosolute species are oligomers of the same protein, $(\partial D/\partial w_i)_\mu = (\mathrm{d}D/\mathrm{d}w_{\mathrm{tot}})_\mu$, which is approximately equal to 0.27 for human IgG (*13*).

The apparent buoyant molar mass of each i-mer is calculated according to the following equation (*5*):

$$\overline{M^*_{\mathrm{app}}} = \underline{A}^{-1}\overline{M^*} \tag{9a}$$

where $\overline{M^*_{\mathrm{app}}}$ denotes a column vector of $M^*_{\mathrm{i,app}}$, $\overline{M^*}$ a column vector of M_i^*, and $\underline{A}$ a square matrix whose elements are given by

$$A_{ij} = \frac{\partial \mu_i}{\partial \rho_j} = \delta_{ij} + \rho_j\left(\frac{\partial \ln \gamma_i}{\partial \rho_j}\right) \tag{9b}$$

where μ_i denotes the chemical potential of the ith species, and δ_{ij} denotes the Kronecker delta (1 if $i = j$ and 0 otherwise). The values of the various $\partial \ln \gamma_i/\partial \rho_j$ are calculated from ρ_i and υ_{eff} using relationships specified by the effective hard particle model, with each species represented by an effective sphere (*1*, *5*, *10*, *14*). The apparent weight-average buoyant molar mass measured experimentally is then calculated according to the following equation (*5*):

$$M^*_{\mathrm{w,app}} = \frac{\sum_i w_i M^*_{i,\mathrm{app}}}{w_{\mathrm{tot}}} \tag{10}$$

Model Calculation of Osmotic Pressure of Nonideal Mixtures of Nondiffusible Solutes. At constant temperature, the Gibbs−Duhem relationship is as follows:

$$V\,\mathrm{d}P = \sum_{i=0}^{n} c_i\,\mathrm{d}\mu_i \tag{11}$$

where V and P denote the volume and pressure, respectively, of the system, and μ_i denotes the chemical potential of species i. Let a solution of composition {c} be separated from the pure solvent (species 0) by a membrane that is permeable only to species 0. The osmotic pressure is the difference between the pressure of the solute and solvent compartments at equilibrium (*12*).

$$\bar{v}_0\,\mathrm{d}\Pi = \sum_{i=1}^{n} c_i\,\mathrm{d}\mu_i \tag{12}$$

where $\bar{v}_0$ denotes the specific volume of solvent. The dependence of the osmotic pressure upon the concentration of each nondiffusible species is then given by

$$\bar{v}_0\left(\frac{\partial \Pi}{\partial c_j}\right)_{\{c\}} = \sum_{i=1}^{n} c_i\left(\frac{\partial \mu_i}{\partial c_j}\right)_{\{c\}} \tag{13}$$

where it is assumed that the contribution from the Donnan effect is negligible, as is the case for proteins in solutions of moderate ionic strength. Consider the following conceptual process for preparing a solution containing final concentrations of c_1^*, c_2^*, ..., c_n^* of n nondiffusible solutes. First, species 1 is added to solvent to a final concentration of c_1^*. Solute addition is performed at constant solution volume by simultaneous removal of the appropriate quantity of solvent. Then species 2 is added to the solution containing a fixed concentration c_1^* to a final concentration c_2^*. Species 3 is then added to the solution containing fixed concentrations c_1^* and c_2^* to a final concentration c_3^*. In a similar fashion, each additional solute species is successively added to its final concentration. Following this protocol, we calculated the osmotic pressure of the final solution by adding up the changes in osmotic pressure accompanying the stepwise addition of each nondiffusible solute species.

$$\Pi(c_1^*, c_2^*, \ldots c_n^*) = \int_0^{c_1^*}\left(\frac{\partial \Pi}{\partial c_1}\right)_{c_{2\ldots n}=0}\mathrm{d}c_1 + \int_0^{c_2^*}\left(\frac{\partial \Pi}{\partial c_2}\right)_{c_1=c_1^*, c_{3\ldots n}=0}\mathrm{d}c_2 + \ldots + \int_0^{c_n^*}\left(\frac{\partial \Pi}{\partial c_n}\right)_{c_{1\ldots n-1}=c^*_{1\ldots n-1}}\mathrm{d}c_n \tag{14}$$

Equations 5, 9b, and 12−14 may be combined to yield the following explicit expression for the osmotic pressure of a solution containing up to three nondiffusible solute species, where concentration is expressed in units of number density ρ (cm^{-3}):

$$\begin{aligned}\bar{\Pi}(\rho_1^*, \rho_2^*, \rho_3^*) = \frac{RT1000}{N_A \bar{v}_0}\Bigg[&\rho_1^* + \rho_2^* + \rho_3^* + \\ &\int_0^{\rho_1^*}\left(\frac{\partial \ln \gamma_1}{\partial \rho_1}\right)_{\rho_{2,3}=0}\mathrm{d}\rho_1 + \int_0^{\rho_2^*}\rho_2\left(\frac{\partial \ln \gamma_2}{\partial \rho_2}\right)_{\rho_1=\rho_1^*, \rho_3=0}\mathrm{d}\rho_2 + \\ &\int_0^{\rho_3^*}\rho_3\left(\frac{\partial \ln \gamma_3}{\partial \rho_3}\right)_{\rho_{1,2}=\rho^*_{1,2}}\mathrm{d}\rho_3 + \rho_1^*\int_0^{\rho_2^*}\left(\frac{\partial \ln \gamma_1}{\partial \rho_2}\right)_{\rho_1=\rho_1^*, \rho_3=0}\mathrm{d}\rho_2 + \\ &\rho_1^*\int_0^{\rho_3^*}\left(\frac{\partial \ln \gamma_1}{\partial \rho_3}\right)_{\rho_{1,2}=\rho^*_{1,2}}\mathrm{d}\rho_3 + \rho_2^*\int_0^{\rho_3^*}\left(\frac{\partial \ln \gamma_2}{\partial \rho_3}\right)_{\rho_{1,2}=\rho^*_{1,2}}\mathrm{d}\rho_3\Bigg]\end{aligned} \tag{15}$$

RESULTS AND DATA ANALYSIS

Sedimentation Equilibrium. The measured dependence of $M^*_{\mathrm{w,app}}$ upon loading concentration is plotted in Figure 2. Each point represents the mean of three replicate determinations. The strong decrease in $M^*_{\mathrm{w,app}}$ with increasing protein concentration is characteristic of nonspecific repulsive protein−protein interactions derived primarily from excluded volume (*15*). Attempts were made to fit the observed dependence of $M^*_{\mathrm{w,app}}$ upon total protein concentration by means of nonlinear least-squares minimization, using a variety of different self-association schemes, together with the treatment of solution nonideality described above, as described in Zorrilla et al. (*5*). The two simplest schemes, no self-association and monomer−dimer self-association,

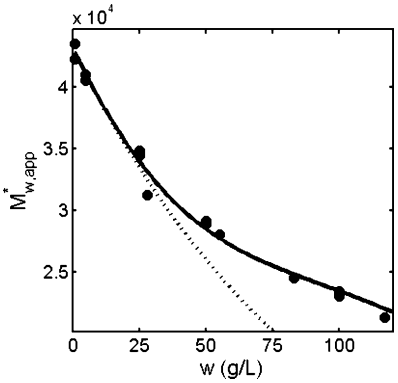

FIGURE 2: Apparent weight-average buoyant molar mass of IgG plotted as a function of protein concentration. The solid curve is the best fit of eq 10, assuming only trimer formation, with log $K_3^0 = 5.0$ and $\upsilon_{eff} = 1.3$ cm^3/g. The dashed curve is calculated with the same value of υ_{eff}, setting $K_3^0 = 0$.

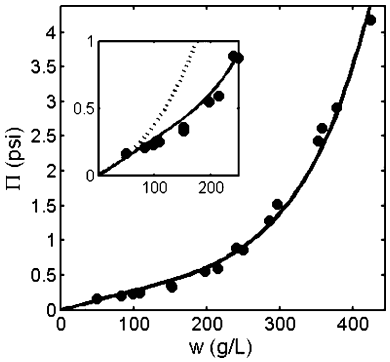

FIGURE 3: Osmotic pressure of IgG plotted as a function of protein concentration. Points: data of Yousef et al. (*7*). The solid curve is the best fit of eq 15, assuming a monomer−trimer asssociation, with the best-fit parameter values log $K_3^0 = 5.45$ and $\upsilon_{eff} = 1.2$ cm^3/g. The dashed curve is calculated with the same value of υ_{eff}, setting $K_3^0 = 0$. The best-fit curves calculated for other association schemes indicated in Table 1 are almost indistinguishable from those plotted.

were unable to fit the data to within experimental precision. The simplest model capable of fitting the data to within experimental precision was a monomer−trimer self-association scheme, suggesting a cooperative self-association mechanism.[2] The dependence of $M^*_{w,app}$ upon w_{tot}, calculated using the best-fit parameter values given in the figure caption, is plotted together with the data in Figure 2. Also plotted in Figure 2 (dashed curve) is a hypothetical dependence of $M^*_{w,app}$ upon w_{tot} calculated on the assumption that the 160 000 MW monomer does not self-associate, that is, taking into account only nonspecific repulsive interactions.

Osmotic Pressure. Yousef et al. (*7*) have measured the concentration dependence of the osmotic pressure Π of bovine IgG in 0.13 M Cl solution over an extremely broad range of concentration. Their results are plotted in Figure 3. Attempts were made to fit the observed dependence of Π on w_{tot} by means of nonlinear least-squares minimization, using a variety of self-association schemes together with the treatment of nonideality described above. It was possible to obtain a satisfactory fit to the data with several different schemes with two variable parameters (Table 1), indicating that the osmotic pressure data of this precision do not provide sufficient resolution to discriminate between association schemes. The best fit of a monomer−trimer scheme is plotted together with the data in Figure 3, and the dependence calculated using the alternate schemes indicated in Table 1 with their respective best-fit parameter values are indistinguishable from the plotted curve at this resolution. Also plotted in this Figure (dashed curve, magnified inset) is a hypothetical dependence of Π upon w_{tot} assuming that the 160 000 monomer does not self-associate, taking into account only nonspecific repulsive interactions.

Table 1: Best-Fit Values of Model Parameters Providing Satisfactory Fits of Eq 15 to the Osmotic Pressure Data of Yousef et al. (*7*) and Eq 10 to the Sedimentation Equilibrium Data Reported Here, Assuming Various Association Schemes

association scheme	experiment	M_1	log K_n^0	υ_{eff} (cm^3/g)
none	osmotic pressure	292 000		1
monomer−dimer ($n = 2$)	osmotic pressure	160 000 (constrained)	3.8	1
monomer−trimer ($n = 3$)	osmotic pressure	160 000 (constrained)	5.45	1.2
	sedimentation equilibrium	160 000 (constrained)	5	1.3

DISCUSSION AND SUMMARY

Knowledge of the state of association of a biological macromolecule under a particular set of experimental conditions is essential for understanding its time-dependent and steady-state behavior and function under those conditions. We emphasize that the state of association of a protein in concentrated solution cannot be reliably inferred from experiments conducted in a dilute solution or in a solution free of other macromolecular species that might be present under physiological or formulation conditions (*1*, *3*).

The most significant finding of the present work is that the concentration dependence of both sedimentation equilibrium and osmotic pressure are quantitatively consistent with a single scheme for weak equilibrium self-association of IgG that is detectable only at protein concentrations exceeding ~30 g/L. Fitting of the respective models to each data set yields similar estimates of the magnitude of repulsive nonideal interactions (as parametrized in the value of υ_{eff}) and in the value of the monomer−trimer association equilibrium constants, which differ by less than a factor of 3. The best-fit monomer−trimer equilibrium association constant ($1-3 \times 10^5$ M^{-2}) corresponds to a standard state free energy change of ca. −8 kcal/mol or a pairwise attractive intermolecular binding energy of ca. −4 kcal/mol, which is comparable in magnitude to previously reported free energies of nonspecific association in aldolase and ovalbumin under similar experimental conditions (*4*). The best-fit value of υ_{eff}, 1.2−1.3 cm^3/g, is indicative of a moderate degree of electrostatic repulsion acting between individual IgG molecules (*16*), consistent with a net negative charge due to the difference between the range of isoionic pH exhibited by polyclonal IgG (5.8−7.3) (*17*) and the pH of measurement (7.4). We speculate that this combination of weak, nonspecific association and electrostatic repulsion may be a fairly

[2] While a monomer−dimer−trimer self-association scheme could fit the data, species distributions calculated using the best-fit association constants indicated that at most, dimers could constitute <5% of total protein. Hence, this model is essentially equivalent to a monomer−trimer model. Models specifying significant quantities of species larger than a trimer are incompatible with the data.

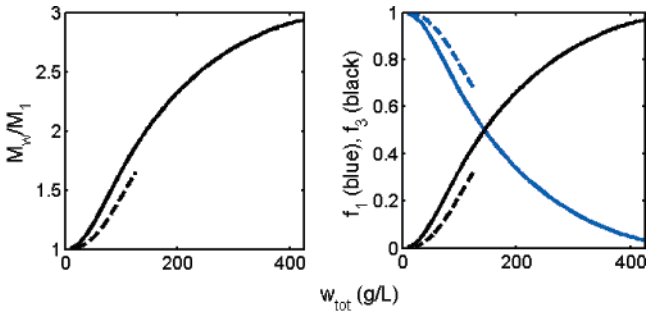

FIGURE 4: Weight average degree of association (left panel) and mass fractions of monomer and trimer (right panel) plotted as a function of total protein concentration. Solid curves: estimated from the modeling of osmotic pressure data. Dashed curves: estimated from the modeling of sedimentation equilibrium data.

common consequence of short-ranged attractive multipolar electrostatic interaction between localized constellations of mixed charge on the surfaces of interacting protein molecules, even though both molecules can have identical net charge and hence repel each other at longer distances.

Taking into account both remarked and unremarked differences in the protein solutions used in the two sets of experiments[3] and the approximate treatment of nonspecific repulsive protein−protein interactions in highly concentrated protein solutions, the degree of agreement between the results of these two analyses is quite good. We conclude that analysis of sufficiently precise and extensive data using the approximate models presented here can provide a realistic semiquantitative assessment of the nature and extent of weak self-association in a concentrated protein solution, provided that attention is paid to the limitations of the effective hard particle model for nonideal behavior (*1*).

The values of the weight-average molar mass and the mass fractions of monomer and trimer, calculated using both sets of best-fit parameter values, are plotted as functions of total protein concentration in Figure 4. According to our interpretation of the combined results, the fraction of total protein present as trimer is approximately 1/3 at a concentration of 100 g/L and over 1/2 at a concentration of 200 g/L. This significant degree of oligomer formation may have important biological consequences. For example, intravenous administration of an engineered antibody biopharmaceutical is an increasingly common treatment for a wide range of diseases (*18*). This procedure generally involves the injection of very concentrated (50−200 g/L) formulations of the therapeutic antibody. Additionally, certain diseases such as smoldering multiple myeloma are associated with highly elevated (>30 g/L) serum IgG concentrations (*19*). The presence of IgG oligomers under these conditions could have immunological consequences because it has been reported that immune response may be greatly enhanced by protein aggregation (*20*−*22*).

A weakly associating protein can be induced to associate more strongly in the presence of high concentrations of unrelated macromolecular cosolutes (*23*−*25*). The technique of nonideal sedimentation equilibrium employed in the present study may be utilized with minor modification (*23*, *26*) to characterize the enhancement or possible inhibition of antibody aggregation that may result from nonspecific interaction between antibody and polymeric adjuvants or serum proteins such as albumin, and studies of these heterologous interactions are currently underway.

[3] For example, human vs bovine IgG and 0.15 M Cl^- vs 0.13 M Cl^- buffers.

ACKNOWLEDGMENT

We thank Dr. Peter McPhie (NIH) for a critical review of the initial draft of this article and the anonymous reviewers for helpful suggestions.

REFERENCES

1. Hall, D., and Minton, A. P. (2003) Macromolecular crowding: qualitative and semiquantitative successes, quantitative challenges, *Biochim. Biophys. Acta 1649*, 127−139.
2. Shire, S. J., Shahrokh, Z., and Liu, J. (2004) Challenges in the development of high protein concentration formulations, *J. Pharm. Sci. 93*, 1390−1402.
3. Minton, A. P. (1998) Molecular crowding: analysis of effects of high concentrations of inert cosolutes on biochemical equilibria and rates in terms of volume exclusion, *Methods Enzymol. 295*, 127−149.
4. Muramatsu, N., and Minton, A. (1989) Hidden self-association of proteins, *J. Mol. Recognit. 1*, 166−171.
5. Zorrilla, S., Jiménez, M., Lillo, P., Rivas, G., and Minton, A. P. (2004) Sedimentation equlibrium in a solution containing an arbitrary number of solute species at arbitrary concentrations: theory and application to concentrated solutions of ribonuclease, *Biophys. Chem. 108*, 89−100.
6. Harn, N., Allan, C., Oliver, C., and Middaugh, C. R. (2007) Highly concentrated monoclonal antibody solutions: direct analysis of physical structure and thermal stability, *J. Pharm. Sci. 96*, 532−546.
7. Yousef, M. A., Datta, R., and Rodgers, V. G. J. (1998) Free-solvent model of osmotic pressure revisited: application to concentrated IgG solution under physiological conditions, *J. Colloid Interface Sci. 197*, 108−118.
8. Darawshe, S., Rivas, G., and Minton, A. P. (1993) Rapid and accurate microfractionation of the contents of small centrifuge tubes: application in the measurement of molecular weight of proteins via sedimentation equilibrium, *Anal. Biochem. 209*, 130−135.
9. Rivas, G., Ingham, K. C., and Minton, A. P. (1994) Ca(2+)-linked association of human complement C1s and C1r, *Biochemistry 33*, 2341−2348.
10. Chatelier, R. C., and Minton, A. P. (1987) Sedimentation equilibrium in macromolecular solutions of arbitrary concentration. I. Self-associating proteins, *Biopolymers 26*, 507−524.
11. Snoussi, K., and Halle, B. (2005) Protein self-association induced by macromolecular crowding: a quantitative analysis by magnetic relaxation dispersion, *Biophys. J. 88*, 2855−2866.
12. Eisenberg, H. (1976) *Biological Macromolecules and Polyelectrolytes in Solution*, Clarendon Press, Oxford, U.K.
13. Durschlag, H. (1986) Specific Volumes of Biological Macromolecules and Some other Molecules of Biological Interest, in *Thermodynamic Data for Biochemistry and Biotechnology* (Hinz, H.-J., Ed.) pp 45−128, Springer-Verlag, Berlin.
14. Minton, A. P. (2007) Static light scattering from concentrated protein solutions. I. General theory for protein mixtures and application to self-associating proteins, *Biophys. J.*, in press.
15. Ross, P. D., Briehl, R. W., and Minton, A. P. (1978) Temperature dependence of nonideality in concentrated solutions of hemoglobin, *Biopolymers 17*, 2285−2288.
16. Minton, A. P. (1995) A molecular model for the dependence of the osmotic pressure of bovine serum albumin upon concentration and pH, *Biophys. Chem. 57*, 65−70.
17. Schultze, H. E., and Heremans, J. F. (1966) *Molecular Biology of Human Proteins*, Vol. 1, Table 41, p 222, Elsevier, Amsterdam.
18. Dani, B., Platz, R., and Tzannis, S. T. (2007) High concentration formulation feasibility of human immunoglobulin G for subcutaneous administration, *J. Pharm. Sci. 96*, 1504−1517.
19. Rajkumar, S. V., Lacy, M. Q., and Kyle, R. S. (2007) Monoclonal gammopathy of undetermined significance and smoldering multiple myeloma, *Blood Rev.*, in press.

20. Moore, W. V., and Leppert, P. (1980) Role of aggregated human growth hormone (hGH) in development of antibodies to hGH, *J. Clin. Endocrinol. Metab. 51*, 691−697.
21. Chirino, A. J., Ary, M. L., and Marshall, S. A. (2004) Minimizing the immunogenicity of protein therapeutics, *Drug Discovery Today 9*, 82−90.
22. Hermeling, S., Schellekens, H., Coen, M., Gebbink, M. F., Crommelin, D. J., and Jiskoot, W. (2006) Antibody response to aggregated human interferon alpha-2b in wild-type and transgenic immune tolerant mice depends upon type and level of aggregation, *J. Pharm. Sci. 95*, 1084−1096.
23. Rivas, G., Fernandez, J. A., and Minton, A. P. (1999) Direct observation of the self-association of dilute proteins in the presence of inert macromolecules at high concentration via tracer sedimentation equilibrium: theory, experiment, and biological significance, *Biochemistry 38*, 9379−9388.
24. Rivas, G., Fernandez, J. A., and Minton, A. P. (2001) Direct observation of the enhancement of noncooperative protein self-assembly by macromolecular crowding: indefinite linear self-association of bacterial cell division protein FtsZ, *Proc. Natl. Acad. Sci. U.S.A. 98*, 3150−3155.
25. Del Alamo, M., Rivas, G., and Mateu, M. G. (2005) Effect of macromolecular crowding agents on human immunodeficiency virus type 1 capsid protein assembly in vitro, *J. Virol. 79*, 14271−14281.
26. Rivas, G., and Minton, A. P. (2004) Non-ideal tracer sedimentation equilibrium: a powerful tool for the characterization of macromolecular interactions in crowded solutions, *J. Mol. Recognit. 17*, 362−367.

BI7005515